Hindawi
Advances in Materials Science and Engineering
Volume 2022, Article ID 2177630, 15 pages
https://doi.org/10.1155/2022/2177630

Research Article

Microbial Growth and Calcium Carbonate Nucleation Properties in Mineral Admixtures

Qiang Jin,[1,2] **Manxu Zhou**,[1] **Lin Zhu**,[1] **Hanlong Liu**,[1] **and Fuhao Zhu**[1]

[1]*College of Hydraulic, and Civil Engineering, Xinjiang Agricultural University, Urumqi, Xinjiang 830052, China*
[2]*Xinjiang Key Laboratory of Hydraulic Engineering Security and Water Disasters Prevention, Urumqi, Xinjiang 830052, China*

Correspondence should be addressed to Hanlong Liu; xjauhudi@xjau.edu.cn

Received 26 March 2022; Revised 22 May 2022; Accepted 24 May 2022; Published 6 June 2022

Academic Editor: Hany Abdo

In this study, steel slag powder and fly ash were used as reinforcement and modification materials, and their effects on the growth, survival, and nucleation of mineral admixtures on bacteria were analyzed. Electrical conductivity, urease activity, and zeta potential tests were conducted, and the results showed that: (1) different mineral environments had different effects on the urease activity of *Sporosarcina pasteurii*. The steel slag powder solution inhibited urease activity, while the fly ash solution promoted urease activity. (2) *S. pasteurii* showed different growth characteristics in different mineral environments, especially in the fly ash solution, which showed higher hydrolysis efficiency, urease activity, and calcium carbonate yield. (3) The zeta potential test results showed that the nucleation of mineral admixtures on bacteria started to occur when the calcium ion concentration in the mineral filtrate was higher than 15 mmol/L. Different calcium ion concentrations showed greater impacts on the nucleation rate of mineral admixtures. The results of this study indicated the adaptability of microorganisms in the steel slag powder and fly ash solutions and the nucleation characteristics of calcium carbonate on the microbial surface, providing a theoretical and experimental basis for the subsequent development of new sand-fixing materials.

1. Introduction

Biomineralization is defined as all biochemical mechanisms for the selective extraction and uptake of elements from the proximal environment of the organism and their incorporation as functional minerals. Microbially induced $CaCO_3$ precipitation is also a key subtheme under biomineralization [1]. Microbial-induced carbonate precipitation (MICP) technology uses microbial, growth, consolidation, and extinction processes to solidify the engineering properties of deserts, soils, and rocks, which have been found in the environment since ancient times. Desertification is a widespread problem worldwide, posing unprecedented and enormous challenges to economic development, social progress, ecological protection, and environmental management. China is experiencing very serious land desertification [2]. In Xinjiang, due to its special aeolian sandy soil, loose, and easily erodible particles, along with large amounts of sand, frequent dust erosion, and a cold environment prone to drought [3], desert microbial mineralization faces new challenges [4]. In the field of sand consolidation, existing studies have focused on hydrogenic sands, such as a river, lake sands, and marine sands. Wind-formed sands, which are formed by wind action, have not been sufficiently comprehensively studied in arid and semiarid regions. In addition, basic research on microbial consolidation and its modification of aeolian sandy soil has been insufficient, and the latter requires further research on the cementation mechanism, key influencing factors, and modification methods of aeolian sandy soil based, on MICP technology [5].

Mitchell and Santamarina [6] used microbial processes to solve problems in geotechnical engineering and proposed that the microbial environment of a single curing action could affect the soil properties. Whiffin et al. [7] used MICP technology to produce sand columns indoors with different sizes to study the ability of the microorganisms to generate calcium carbonate in the pores of the sand columns and

verified the feasibility of using this technique for practical engineering. Dworatzek [8] conducted a field trial study on the reinforcement of soils using MICP based on urea hydrolysis, providing a reference for the advancement of microbial mineralization overlay in deserts. Li et al. [9] showed that the microbial-induced carbonate precipitation (MICP) technology caused the formation of dense aeolian sandy soil, which originally showed no intergranular cohesion, and was significantly stronger after mineralization through the enhancement of intergranular occlusion and association. Cheng and Cord-Ruwisch [10] investigated the effects of sand density, temperature, and pH on the effect of microbial sand curing, and the results showed that high-density sand had higher compressive strength than low-density sand. In addition, acidic (pH = 3.5) and alkaline (pH = 9.5) conditions were not conducive to the improvement in the curing strength of aeolian sandy soil. Cui et al. [11] performed microbial curing of sand mixtures consisting of aeolian sandy soil and standard sands and found that higher porosity and better particle gradation resulted in higher strength. Cheng et al. [12] studied the effect of microbial curing of sand with different saturation levels (20%, 40%, 60%, and 100%) and showed that microbial curing was the most effective for sandy soils with lower saturation (20%). Dejong et al. [13] and Ferris et al. [14] determined that the pH of the solution changed with prolonged microbial curing time, and the production of calcium carbonate crystals was influenced by the pH.

China is the largest iron and steel producer in the world, and a large number of high energy-consuming iron and steel enterprises, as well as their affiliated thermal power plants, often generate large amounts of solid waste such as steel slag and fly ash during the production process [15]. This process is also accompanied by significant pressure to reduce CO_2 emissions. Studies have shown that steel slag and fly ash are rich in potentially active components and their potential cementitious properties in aqueous environments may result in the formation of cementitious substances [16, 17]. Steel slag is rich in calcium and magnesium elements, both of which account for more than 50% of its total content. However, efficient utilization of the rich calcium and magnesium elements in steel slag, as well as addressing the impact of its free calcium oxide (f-CaO), are key issues that need to be addressed to improve its comprehensive utilization. In addition, biotechnology could be used to accelerate the use of solid waste containing calcium and magnesium, such as steel slag to solidify CO_2, while achieving zero-emission steel slag and reducing the pressure of CO_2 emission reduction. This process would also highlight the sustainable development concept of using waste to treat waste and could offer broad application prospects.

Water plays an important role in the growth and mineralization of microorganisms in arid desert environments. Therefore, it is necessary to optimize the water retention properties of sandy soils to provide sufficient water for microbial growth and mineralization. Zhao et al. [18] investigated the effect of fly ash as a sandy soil amendment on the water retention properties of sandy soils. The study showed that the application of fly ash could effectively improve the physical properties of sandy soils, and the water content of the improved sandy soils significantly increased. Pandey and Singh [19] described the effect of fly ash on soil systems and showed that fly ash could be effectively used in poor or sterile soils to improve soil quality and fertility. Akinwumi [20] used different blends of steel slag to improve poorly engineered soils. In addition, Huang et al. [21] used the microscopic analysis of steel slag soil mixes to show that changes in the surface charges of the soil particles caused the mixed steel slag soil structure to be more compact during formation and that the hydration of f-CaO in steel slag during curing was significantly inhibited. At the same time, steel slag and soil wrap around each other, forming a stacking effect and self-compacting effect between particles, thus increasing the strength of the soil. Calcium carbonate nucleation on the surface of bacteria is affected by the environment of added mineral dopants. Bacterial morphology and motility affect the accumulation of calcium on the cell surface. The cell surface permeability has a specific role in the MICP process. Ion transport is reduced due to the accumulation of crystals on the cell surface, thereby reducing the production of extracellular carbonate [22]. However, carbonate ions are produced outside the cell; the environmental pH changes through the action of MICP. This process contributes to the saturation of ions and promotes the formation of $CaCO_3$ [23]. Changes in pH during MICP can reflect the main metabolic effects of biocalcification, and therefore, changes in pH can be used as a physical indicator of MICP [24].

The rate of microbial mineralization is susceptible to the environmental pH, and the ability to adapt will also have an important effect on the mineralization reactions. In this study, steel slag and fly ash were used as modification materials for the microbial curing of aeolian sandy soil, which was centered around the growth and nucleation characteristics of mineral admixtures. The effects of steel slag and fly ash on the growth and nucleation characteristics of mineral admixtures subtilis were analyzed via conductivity, urease activity, and zeta potential tests. Then, the growth, survival, multiplication, and curing properties of *Sporosarcina pasteurii* were characterized based on changes in optical density, solution pH, conductivity, and zeta potential. The effects of the modified materials on the physicochemical properties of *S. pasteurii* were clarified by providing theoretical and experimental data, which were used to support the enhancement of microbial curing effects by the mineral admixtures and the development of new sand fixation materials and technologies.

2. Materials and Methods

2.1. Materials

2.1.1. The Aeolian Sandy Soil. The desert aeolian sandy soil used in the experiment was collected from the Gurbantunggut Desert in Midong District, Urumqi, Xinjiang Uygur Autonomous Region, China. The current appearance of aeolian sandy soil is shown in Figure 1. According to GB/T 50123-1999 soil test method standard, the water content of

Figure 1: Appearance of experimental materials.

natural sand was measured by the drying method, the dry density was measured by the cutting ring method, and the particle size distribution was determined by the sieve test. The dry sand sample (50 g) was put into a wide-mouth flask; pure water was added according to the soil-water ratio of 2:5, stirred on an oscillator for 5 minutes, and then filtered; and then the pH value of the liquid was measured. The water content of natural sand was 0.14%; the dry density was 1.61 g/cm^3; the density of quartz particles was 2.64 g/cm^3; the porosity was 43.2%; and the pH value was 8.36. The sand composition of weathered sandy soil was mostly less than 0.6 mm and 99.2% of the total. The median diameter is 0.15 mm; the uniformity coefficient is 2.08; and the curvature coefficient is 1.11. These results indicate that the weathered sandy soil is sand of uniform grains.

2.1.2. Steel Slag Powder. Steel slag is a by-product of the steel-making process. In this test, hot smothered steel slag provided by Baosteel Group Xinjiang Bayi Iron & Steel Co. Ltd. was selected and ground using a ball mill for 20 minutes to give it a certain degree of water hardness. The particle size distribution of the steel slag powder used in the experiment is shown in Table 1, and according to GB/T8074-2008 cement specific surface area determination method (Burn's method), the specific surface area of steel slag powder is 430 m^2/kg. The main performance indicators of steel slag powder are shown in Table 2.

2.1.3. Fly Ash. Fly ash is a by-product produced during the combustion process of thermal boilers. In this test, the fly ash provided by Xinjiang Hulijiayuan Environmental Protection Technology Co. The particle size distribution of fly ash particles is shown in Table 3, which shows that the particle composition of fly ash is relatively consistent, with coarse fly ash (50–10 μm), mainly accounting for 45.88% of medium powder (10–5 μm), followed by 15.5% of fine powder (<5 μm). The content is 9.12%. The density is 2.40 g/cm^3, and the fineness is 17.1%. According to GB/T 1596-2017 fly ash used for cement and concrete, the fly ash used in the test was type II fly ash with a specific surface area of 450 m^2/kg and a burn loss of 2%. Its main performance indicators for fly ash are shown in Table 2.

Table 1: Particle size distribution of steel slag power.

Particle size (μm)	< 5	< 30	< 70	< 100
Particle size distribution (%)	0.83	53.42	85.23	100

S. pasteurii: *S. pasteurii* were obtained from Shanghai Bioresource Collection Center (NO. ATCC 11859).

Trypticase soy broth (TSB): The culture medium was used from Guangdong Huankai Microbial Sci & Tech. Co. Ltd. The specific composition is shown in Table 4.

2.2. Instruments and Equipment

Pressure steam sterilizer: XFS-280, Zhejiang Xinfeng Medical Apparatus Co. Ltd.

Clean benche: VD-850, Shanghai Lichen Instrument Technology Co. Ltd.

Constant temperature oscillation incubator: ZD-85, Shanghai Lichen Instrument Technology Co. Ltd.

High-precision pH acidity meter: PHS-3E, Shanghai INESA Scientific Instrument Co. Ltd.

Spectrophotometer: 722 N, Shanghai INESA Scientific Instrument Co. Ltd.

Conductivity meter: DDS-307, Shanghai INESA Scientific Instrument Co. Ltd.

Acoustic and electroacoustic spectrometer: DT-310, Dispersion Technology Inc.

The main test instruments are shown in Figure 2.

2.3. Preparation for the Test. The bacterial solutions were prepared by first drawing 1 mL of a bacterial solution with an OD600 value of 2.0, which was then inoculated in a TSB medium and placed in a constant temperature oscillator at 30°C at 170 rpm. The test used three bacterial solutions and five nonbacterial solutions, which are presented in Table 5.

Table 2: Main performance indicators of mineral admixture micronized powder.

Type	Activity index	Chemical composition (%)						
		SiO_2	Al_2O_3	CaO	TFe	MgO	f-CaO	Fe_2O_3
Steel slag powder	0.75	13.11	3.05	42.65	17.5	8.85	1.24	6.82
Fly ash	0.69	54.28	27.16	2.83	—	0.94	—	

Table 3: Particle size distribution of fly ash.

Particle size (μm)	< 5	5–10	10–30	30–50	50–70	70–100	> 100
Particle size distribution (%)	9.12	15.50	24.37	21.51	12.38	9.69	7.43

Table 4: TSB medium components (per liter).

Composition	Quantity per liter of deionized water
Pancreatic digest of casein	17.0 g
Papaic digest of soya bean (soybean)	3.0 g
Sodium chloride	5.0 g
Dipotassium hydrogen phosphate	2.5 g
Glucose monohydrate	2.5 g
Final pH	7.3 ± 0.2

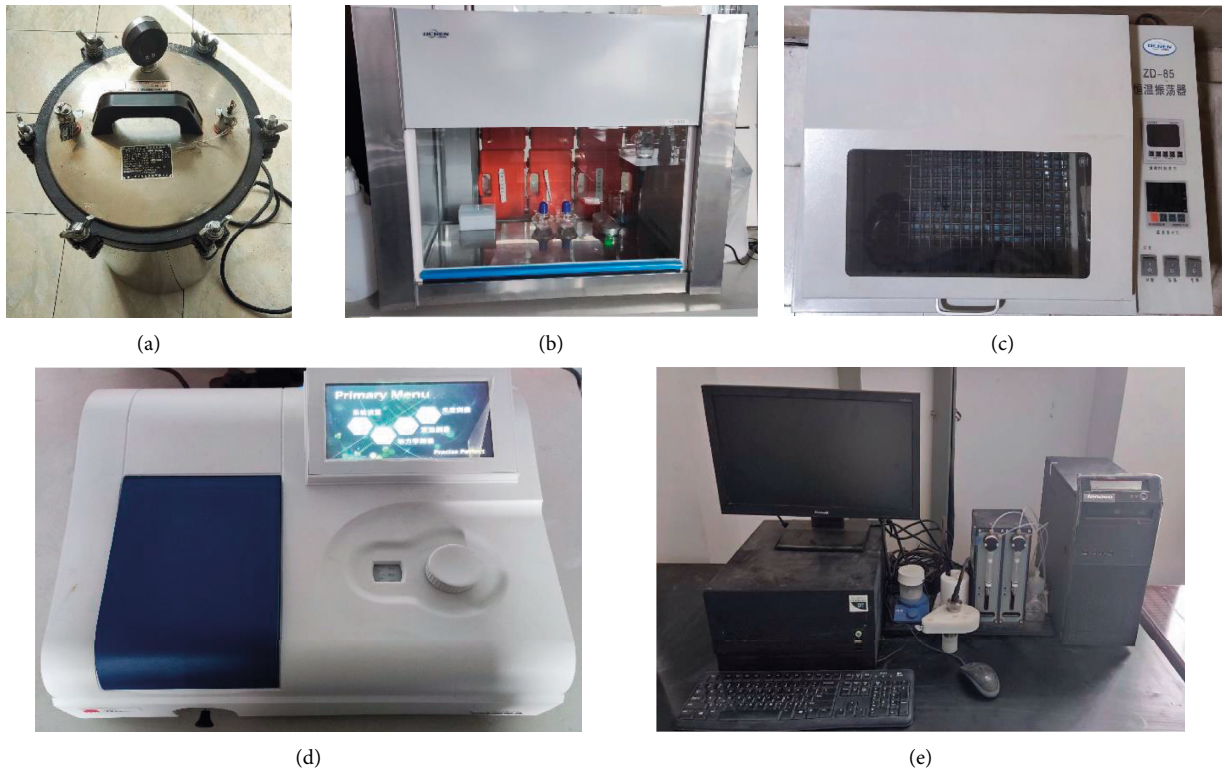

(a) (b) (c) (d) (e)

Figure 2: Main instrumentation images: (a) pressure steam sterilizer, (b) clean benche constant, (c)temperature oscillation incubator, (d) spectrophotometer, and (e) acoustic and electroacoustic spectrometer.

2.4. Testing Procedures

2.4.1. Bacterial Concentration. The bacterial concentration was expressed by measuring the absorbance of the bacterial solution, according to the turbidimetric method. The test was conducted at an ambient temperature of 25°C by pipetting 3 mL of the measured liquid in a cuvette and the spectrophotometer wavelength was adjusted to 600 nm. The test was then initiated by photometric calibration, where the cuvette was placed in the photometer, and the absorbance of the liquid was recorded when the reading was stable [25].

Table 5: Names of the solutions and bacterial solutions.

Solution type	Abbreviation	Preparation method
TSB culture solution	TSB	TSB was mixed with deionized water and then autoclaved.
TSB bacterial liquid	BL	*Sporosarcina pasteurii* was obtained by culturing in a TSB culture medium
Fly ash bacterial liquid	FA BL	FA BL was obtained by culturing the bacteria in a mixture of fly ash and TSB solution.
Steel slag powder bacterial liquid	SSP BL	SSP BL was obtained by culturing the bacteria in a mixture of steel slag powder and TSB solution.
Fly ash filtration liquor	FA	Fly ash was soaked in deionized water for 2 h according to the mass ratio and then filtered
Fly ash mixture	TSB FA	Naming convention followed the mass ratio (i.e., FA2% and FA4%). TSB culture was mixed with the fly ash in a mass ratio and filtered.
Steel slag powder filtration liquor	SSP	Steel slag powder soaked in deionized water for 2 h by mass and filtered.
Steel slag powder mixture	TSB SSP	Naming convention followed the mass ratio (i.e., SSP2%, SSP4%). TSB culture was mixed with the steel slag powder solution in a mass ratio and filtered.

2.4.2. Urease Activity. Bacterial metabolism will produce urease, which catalyzes the hydrolysis of urea. According to the urease catalyzed reaction products of urea hydrolysis, originally nonconductive urea will be hydrolyzed to conductive NH_4^+ and CO_3^{2-}, resulting in a gradual increase in the number of ions in the solution and conductivity of the solution. According to the results of Whiffin [26], the rate of change of conductivity of the solution was linearly correlated with the urease activity in the bacterial solution. In this test, 1 mL of the bacterial solution was added to 9 mL of 1.5 M urea solution at 25°C, and the solution was diluted 10 times. Then, changes in the conductivity of the solution were measured over 5 min. The urease activity of the bacterial solution was calculated as the product of the change in mean conductivity and the dilution factor. The sap urease activity was calculated as follows [27]:

$$U = 11.11 f \,(R2 = 0.9988), \tag{1}$$

where U is the bacterial sap urease activity (mmol/(L·min)) and f is the rate of change of conductivity in the bacterial solution (mS/min).

2.4.3. Solution pH. The pH will significantly affect the growth rate of microorganisms. For the solution pH test, 50 mL of solution was drawn and placed in a calibrated pH meter in the test solution. When the readings were stable, the test was averaged using three consecutive measurements, and the ambient pH of the solution was recorded [28].

2.4.4. Calcium Carbonate Production. An acid wash test was used to calculate the amount of calcium carbonate produced. The solidification solution consisted of a mixture of 0.5 M $CaCl_2$ and 0.5 M urea solution at a 1:1 ratio. First, 1 mL of the test solution was added to 30 mL of the test solution, and the amount of precipitated calcium carbonate was tested at 3, 5, and 7 d. The solid in the conical flask was first rinsed with deionized water and then dried and weighed. Subsequently, the solid product in the conical flask was acid washed with an excess of 0.1 M hydrochloric acid until no air bubbles were produced. Finally, the product was dried and weighed. The amount of calcium carbonate produced was determined according to the difference between the two dry mass values. The yield of calcium carbonate was calculated by

$$\mu = \frac{(G_1 - G_2)}{G_3 \times 100\%}, \tag{2}$$

where G_1 is the dry mass before pickling, G_2 is the dry mass after pickling, and G_3 is the theoretical calcium carbonate production.

2.4.5. Zeta Potential. The zeta potential measures the strength of mutual repulsion or attraction between particles. In this study, this test was carried out using a DT310 potential analyzer to measure the colloidal vibrational current (CVI) and zeta potential of the solution at 25°C. The zeta potential probe was placed in the measured solution, and the zeta potential value was recorded every 2 min.

3. Results and Discussion

3.1. Physical and Chemical Environment of Microbial Mineralization in Desert Environments

3.1.1. pH of Three Types of Material Solutions. The pH had a significant effect on the growth rate of the bacteria during windblown sand consolidation. This test was carried out using the quadratic method using wind-bound sand, steel slag powder, and fly ash as the raw materials, which were filtered through a 100 mesh screen. First, 120 g ± 0.01 g of the sample was weighed and placed into a 500 mL beaker, and 300 mL of deionized water was added. Then, the beaker was sealed and stirred rapidly with a stirrer for 5 min and allowed to stand for 30 min. The pH of the solution was tested with a pH meter, and the pH value was read once the pH meter reading stabilized. The test was performed every 30 min, and an average of 3 consecutive measurements were obtained, for a total time of 180 min. The pH values of the three types of materials are shown in Figure 3, showing that the solutions of all three materials tested were alkaline. The pH of the wind-deposited sand was between 9.6 and 10. The pH value of the fly ash filtrate was between 11.8 and 12.5. The high alkalinity of the fly ash solution is due to the fact that the ions present in the aqueous solution of fly ash are mostly Ca^{2+}

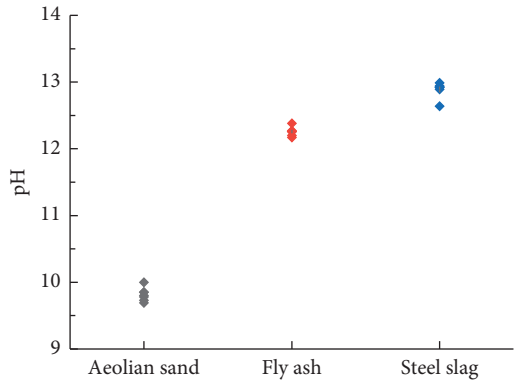

Figure 3: Three types of material pH values.

and OH^- making the solution highly alkaline [29]. The filtrate of steel slag was measured experimentally to be between 12.5 and 13. The high alkaline environment of the steel slag filtrate is caused by the weathering of the steel slag [30]. As a result of the slow hydration process of the steel slag powder and fly ash used, the alkaline substances in the system were slowly released; therefore, the range and values of the pH changes were small [31].

3.1.2. Ca^{2+} Concentration and pH of the Steel Slag Powder and Fly Ash Solutions. When 2%–10% of the utilized steel slag powder and fly ash were used as a mass replacement for the windblown sand, the Ca^{2+} concentrations and pH values of the solutions changed, as shown in Figure 4. The solution Ca^{2+} concentration of the mixed material showed a gradual increase, with an increasing replacement rate. The increase in Ca^{2+} concentration of the solution was more pronounced for the steel slag powder, with variations in the range of 10–31 mmol/L. The variations in solution Ca^{2+} concentration of the fly ash blend were not significant.

3.2. Growth Characteristics of the Microorganisms in Different Mineral Environments

3.2.1. Bacterial Urease Activity in Different Mineral Solutions. The conductivity parameter characterizes the total concentration of free-state ions in a solution. In this work, the decomposition of urea and complex ion reactions in the bacteriological solution were expressed in real time according to the changes in conductivity. This test was designed for three types of solutions—windblown sand, SSP, and FA—and each solution was configured with 50 mL. First, 1 mL of bacterial solution (OD_{600} of 2.0) and 0.9 g of urea were added to the solution, and the conductivity of the solution was monitored in real time using a conductivity meter. The test was recorded once per minute, five times, and the test results are shown in Figure 5. (In the figure, −1 indicates conductivity without the addition of the bacterial solution, and 0 indicates conductivity after the addition of the bacterial solution.)

As shown in Figure 5, the conductivities of the bacterial and FA solutions showed the same change trend. The

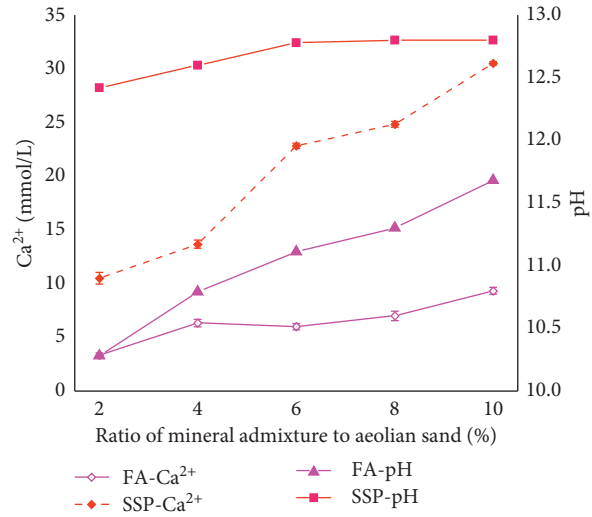

Figure 4: Variations in Ca^{2+} concentration and pH of the steel slag powder and fly ash solutions with different replacement rates.

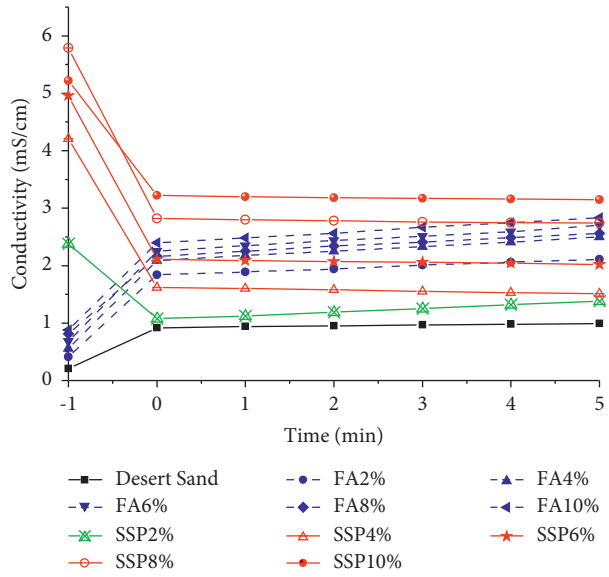

Figure 5: Changes in the conductivity of the bacteria in different mineral solutions for 5 min.

conductivity of the solution was low during the initial stage and increased quickly after the addition of the solution, reaching 270%–450%; then the conductivity trend slowly increased from 0 to 5 min. The conductivity of the SSP solution showed different change patterns, with high conductivity during the initial stage and a rapid drop in conductivity after the addition of the bacterial solution, where the conductivity dropped at 0 min, reaching 38%–61%. The conductivity of the SSP2% solution showed a slowly increasing trend from 0 to 5 min; however, SSP4%, SSP6%, SSP8%, and SSP10% all showed a slowly decreasing trend.

Figure 6 shows that the TSB bacterial liquid (BL) was found in the FA and SSP solutions, and urease activity showed a large difference. BL in FA solution urease activity

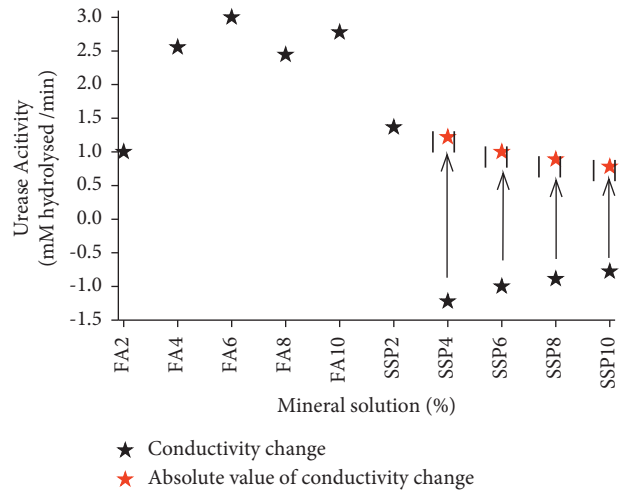

FIGURE 6: Urease activity of the bacteria in different mineral solutions.

was higher, and when fly ash doping was greater than 2%, urease activity noticeably increased. BL in SSP solution conductivity decreased rapidly, indicating that the total number of solution ions decreased. The conductivity of the SSP solution at 5 min showed a decreasing trend, from SSP2% to SSP10%, when the conductivity changes could be observed. As the steel slag powder in the admixture increased, bacterial solution urease activity showed a slowly decreasing trend.

The experimental phenomena during the test also responded to the different behavior of the solution when the bacterial solution was added to the bacterial, steel slag powder, and fly ash solutions as follows:

(1) When the bacteria were added to the aeolian sandy soil filtration liquor, the solution did not change significantly and was relatively clear.

(2) When the bacteria were added to each dose of FA solution, slight white cloudiness gradually appeared in the solution, and white precipitate appeared at the bottom of the solution after 12 h.

(3) When the bacteria were added to the 2% replacement rate (SSP2%) solution, the solution showed a similar phenomenon as the FA solution.

(4) When the bacteria are added to the SSP solution with a replacement rate of 4% or greater (SSP4%–SSP10%), the solution rapidly produced a white flocculent material with the addition of the bacterial solution. A white precipitate with varying degrees also appeared at the bottom of the solution after 12 h.

According to the mineralization mechanism of the microbially induced calcium carbonate production, the decomposition of urea in the solution generated NH_4^+ and CO_3^{2-} from urease, thus substantially increasing the ionic concentration in the solution, which macroscopically manifested as a rapid increase in conductivity. In the steel slag powder solution (SSP), the Ca^{2+} concentration in the solution increased with increases in steel slag powder admixture, and when the Ca^{2+} in the solution reached a certain concentration, the water-soluble organic matter with a negative charge at the interface of the bacterial cell membrane continuously chelated Ca^{2+} in the solution [31]. In addition, CO_3^{2-} was formed via bacterial enzymatic digestion, generating $CaCO_3$ crystals with Ca^{2+} on the cell surface. This reaction process led to a reduction in the number of conductive ions in the solution, resulting in a significant decrease in conductivity and the appearance of more white flocculent material in the solution. The white flocculent gradually settled at the bottom of the container, forming a white precipitate, and subsequent tests indicated that it was primarily composed of $CaCO_3$.

3.2.2. Effect of Bacteria on the pH of Different Mineral Solutions. pH is one of the most important parameters that will affect the growth and development of microorganisms, and the pH level will affect urease activity, the rate of nutrient utilization, and the cell concentration of *S. pasteurii*. The content of soluble mineral components in the SSP and FA solutions at different dosing conditions had a large effect on the pH; thus, it affected the synergistic curing of steel slag powder and fly ash with *S. pasteurii*.

The following two subcases were set up to investigate the effect of bacteria on the pH values of the SSP and FA solutions:

Scheme 1. A test was carried out by adding 1 mL of bacterial solution ($OD_{600} = 2.0$) and 0.9 g of urea at different replacement rates of SSP and FA solutions, respectively. This test was conducted using a pH meter to record the pH changes after 1 minute. The test results are shown in Figure 7(a).

According to Figure 7(a), the pH of the SSP solution was essentially maintained between 12.4 and 12.6 at different replacement rates. The pH of the SSP2% solution with the addition of bacterial solution quickly dropped to 9.75, while the SSP (4%–10%) solutions all showed a small decrease in pH, and remained between 11.9 and 12.5.

However, the pH of the FA solution remained between 10.3 and 11.7 for the different replacement rates, while the pH of FA added to the bacterial solution (2%–10%) quickly dropped to between 9.4 and 9.5.

As shown in Figure 7(b), the bacteriological solution had different degrees of influence on the pH of the SSP solution at the different steel slag powder blending levels. Specifically, the pH of the solution showed the greatest change in a steel slag powder replacement rate of 2%. The effect of the bacterial solution on the pH of FA under different fly ash blending conditions also showed a gradual increase.

Scheme 2. To further investigate the effect of bacteria on the pH of the SSP solution and FA solution for a long period, an experiment was conducted by adding 1 mL of bacterial solution ($OD_{600} = 2.0$) and 0.9 g of urea to a solution of steel slag powder and fly ash with a replacement rate of 10%. The test was carried out using a pH meter to record the pH changes, and the pH of the solution was recorded every

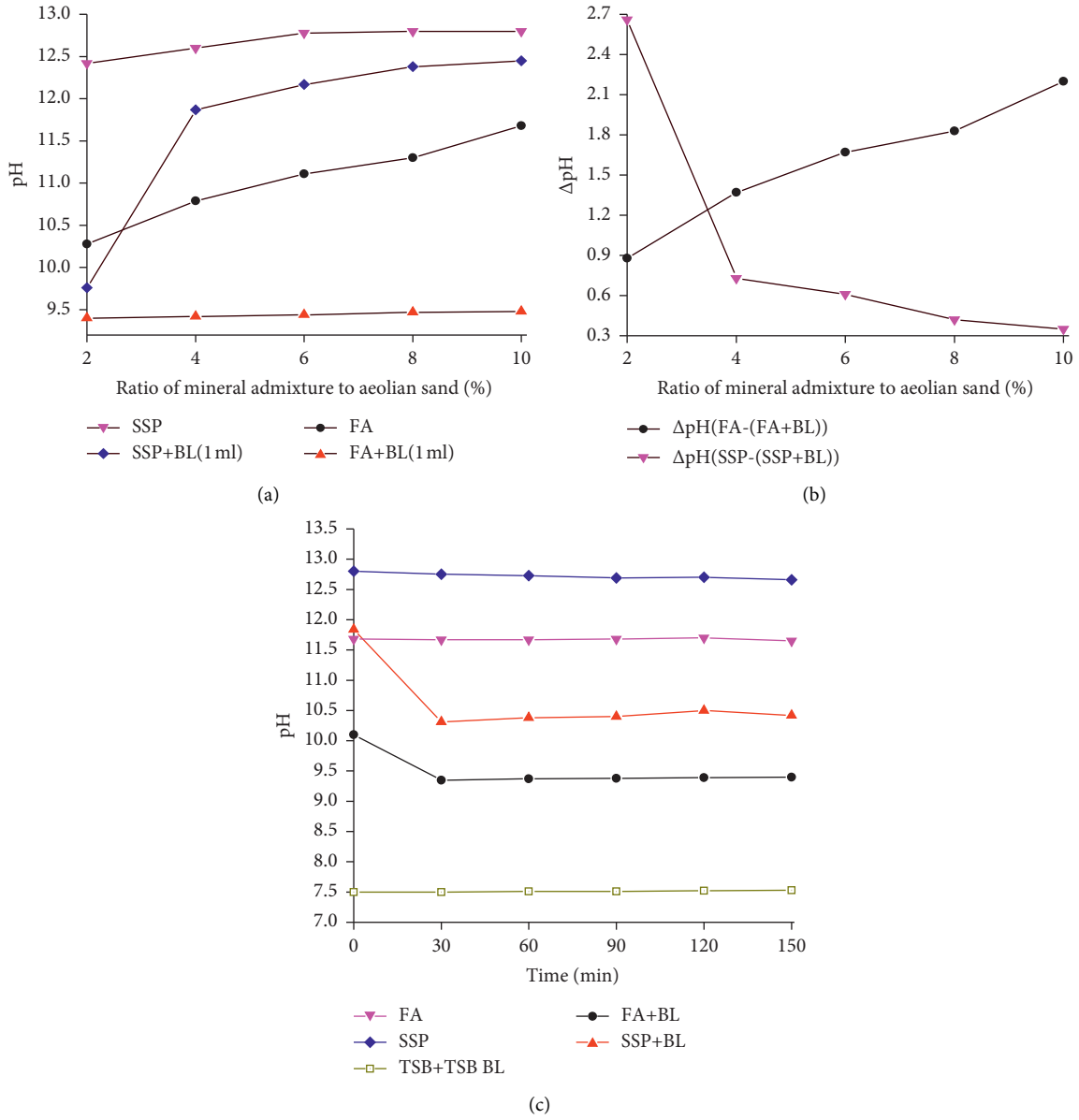

Figure 7: Effect of bacteria on the solution pH under different doping conditions: (a) effect of bacteria on the solution pH under different dosing conditions (1 min), (b) change in solution pH under different dosing conditions (1 min), and (c) effect of the bacterial solution on the pH of the solution.

30 min a total of 5 times. The test results are shown in Figure 7(c).

According to Figure 7(c), the pH values of the SSP and FA solutions without the addition of the bacterial solution did not change significantly; the pH of the FA solution ranged from 11.5 to 12, while the pH of the SSP solution ranged from 12.5 to 13. The pH values of the SSP and FA solutions with the addition of the bacterial solution decreased significantly over 30 min, indicating that the solutions became less alkaline. Additionally, the pH of the FA solution decreased to between 9.3 and 9.6, while the pH of the SSP solution decreased to between 10.3 and 10.5. After 30 min, the pH stabilized after FA and SSP, while the pH of BL in the TSB medium was essentially stable at 7.5.

Urease, which is produced by microbial activity, can catalyze the hydrolysis of urea in urea solutions, causing a series of reactions to occur in the solution, according to the following reactions [32]:

$$NH_2 - CO - NH_2 + H_2O \longrightarrow \text{urease} \longrightarrow NH_3 + NH_2COOH, \quad (3)$$

$$NH_2COOH + H_2O \leftrightarrow H_2CO_3 + +NH_3, \quad (4)$$

$$H_2CO_3 \leftrightarrow HCO_{3^-} + H^+, \quad (5)$$

$$NH_3 + H_2O \leftrightarrow NH_4 + OH^-, \quad (6)$$

$$Ca^{2+} + HCO_{3^-} + OH^- \leftrightarrow CaCO_3\downarrow + H_2O. \quad (7)$$

The change in pH in a conventional soil solution depends mainly on the change in the equilibrium of the reaction in reactions (4) and (5). Carbamate spontaneously hydrolyses to produce carbonic acid and ammonia (2), which itself hydrolyses according to reactions in reactions (4) and (5) with equilibrium constants of pK1 6.3 and pKa 9.3, respectively. Based on the equilibrium constants in this state, it is clear that there will be a net increase in soil pH [33]. However, in the present trial, by comparing Figures 7(a) and 7(c), we found that the bacteria had different levels of influence on the pH values of the SSP and FA solutions. When the pH of the bacterial living environment was higher than 9, the higher amount of OH^- in the solution promoted reactions (4), causing it to proceed in the positive direction. This increased the H^+ concentration, which was manifested as a decrease in pH. However, the pH of the SSP solution during the test was between 12.5 and 13, and a higher pH reduced the urease activity of the bacteria, which affected the efficiencies of reactions (1) and (5) to proceed in the positive direction. When the bacteria were added to the SSP solution, OH^- in the solution promoted the reactions of reactions (4) and (6), causing them to proceed in the positive direction, which lowered the pH. However, the accumulation of $CaCO_3$ crystals due to the adsorption of Ca^{2+} in solution on the bacterial surface may affect the reduced permeability of the cell membrane, further reducing the efficiency of bacterial hydrolysis. This process reduces the reaction rate (1) and leads to a reduction in the ability of the bacteria to regulate the alkaline environment of the SSP solution. In the test, the pH of the FA solution was between 11.5 and 12, and the higher amount of OH^- in the solution promoted reactions (4) and proceeded in the positive direction, causing the H^+ concentration to increase and the pH to decrease. However, $Ca_2{}^+$ content in the FA solution was low; therefore, this condition had less effect on the efficiency of bacterial hydrolysis. As hydrolysis continued to occur, reaction (6) gradually stopped, and reactions (4) and (5) gradually equilibrated when the pH of the solution was 9.5; thus, the pH of the solution reached a steady state.

3.2.3. Growth Characteristics of the Bacteria in Different Mineral Solutions. The aforementioned conductivity tests showed that when steel slag powder and fly ash were used as reinforcement materials for wind-bound sand curing, *S. pasteurii* could maintain good urease activity under these conditions and provide an enhancing effect. However, the aqueous solution of steel slag powder and fly ash was alkaline with pH values of 10–13, and the alkaline environment had a detrimental effect on the growth, reproduction, and urease activity of *S. pasteurii.*

To further determine the adaptation of *S. pasteurii* to a highly alkaline and complex environment, *S. pasteurii* was incubated in an aqueous TSB medium containing TSB SSP and TSB FA solutions, to analyze the growth and multiplication of *S. pasteurii* in this type of environment. The results of the previous tests showed that the suspension and hydration characteristics of the steel slag powder and fly ash in the aqueous solution affected OD_{600}. As a result, the TSB SSP solution without microbial inoculation and the aqueous TSB medium solution with TSB FA solution were set up as the control groups, where BL was the cultured bacteria in the TSB medium. The bacterial solution was prepared by extracting 1 mL of the bacterial solution with an OD_{600} of 2.0, which was inoculated in the corresponding solution and placed in a constant temperature oscillator at 30°C and 170 rpm.

As shown in Figure 8, the OD_{600} of the three solutions containing bacteria grew continuously, with rapid growth in OD_{600} after 2 h, and logarithmic bacterial growth with vigorous metabolism between 2 and 12 h. The concentration of the bacterial solution remained stable after 12 h and entered the stabilization phase. A comparison of the BL, ΔOD_{600} (TSB SSP), and ΔOD_{600} (TSB FA) curves indicated that the bacteria were well adapted to the cultural environments of both solutions and showed good growth characteristics. The OD_{600} values of the bacteria in TSB FA were consistently higher than the other two solutions, which were possibly related to the higher OD_{600} values as a result of the smaller fly ash particles and their apparent suspension characteristics. Therefore, further testing was required to determine why the bacteria were better adapted to TSB FA than the other two solutions.

3.2.4. Analysis of Bacterial Urease Activity in the Different Culture Environments. The SSP BL, FA BL, and BL were used to test their urease activity in deionized water (W) and FA and SSP solutions.

The test protocol consisted of 1 mL of bacterial solution and 0.9 g of urea, which were added to the 3 solutions, and the solution conductivities were recorded in real time using a conductivity meter. Then, the urease activity was calculated. The specific urease activity test solution protocol scheme is shown in Table 6, and the test results are shown in Figure 9.

As shown in Figure 9, the urease activities of BL, SSP BL, and FA BL showed large differences after they were added to the corresponding test solutions. BL showed some differences in urease activity in the W and FA solutions, with a higher activity in the FA solution and close to average urease activity in the SSP and W solutions. FA BL showed a high urease activity value of 2.6 in the FA solution, which was much higher than the results of the other conditions and was twice that of average urease activity. The activity of W was also higher than the average urease activity; SSP BL had slightly higher urease activity than the average urease activity in the SSP solution; and the activity in W was close to the average urease activity.

Greater urease activity was caused by the higher-than-average urease activity of BL in the FA solution, combined with pH values of the FA solution between 10.3 and 10.5 shown in Figure 7(c), as well as an alkaline environment that was optimal for microbial enzymes to promote urea hydrolysis reactions [31].

FA BL had the highest urease activity in the FA solution, up to 2.6 mmol/(L·min), indicating that FA BL cultured in the fly ash solution showed great adaptability improvements

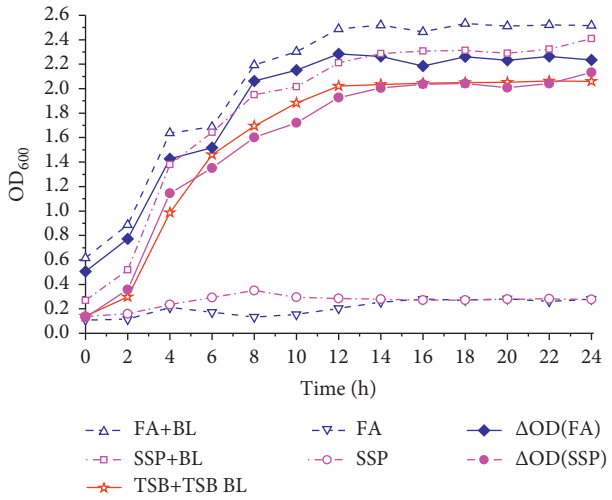

Figure 8: Growth characteristics of *Sporosarcina pasteurii* in aqueous solutions containing fly ash and steel slag powder.

Table 6: Urease activity test solution protocol.

Group number	Test combinations
BL + W	TSB culture bacteria (BL) + deionized water (W)
FA BL + W	Fly ash culture bacteria (FA BL) + deionized water (W)
SSP BL + W	Steel slag powder culture bacteria (SSP BL) + deionized water (W)
BL + FA	TSB culture bacteria (BL) + fly ash test solution (FA)
FA BL + FA	Fly ash culture bacteria (FA BL) + fly ash test solution (FA)
BL + SSP	TSB culture bacteria (BL) + steel slag powder test solution (SSP)
SSP BL + SSP	Steel slag powder culture bacteria (SSP BL) + steel slag powder test solution (SSP)

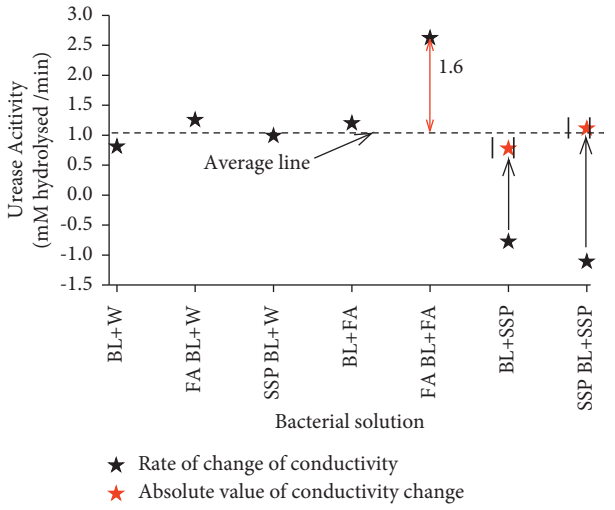

Figure 9: Urease activity distribution map.

to the fly ash solution. Therefore, FA BL greatly accelerated the hydrolysis rate of urease in the FA solution, and the number of ions in the solution increased rapidly.

After BL and SSP BL were added to SSP, the conductivity of the solution decreased rapidly, indicating that the total number of ions in the solution decreased. When BL and SSP BL were dropped into the SSP solution, a milky suspended substance was observed. After 12 h, more white substance precipitated at the bottom of the solution, and obvious precipitates and suspended matter were found in W and FA. Figure 4 shows that the number of calcium ions in the SSP solution was much higher than in the FA solution. According to the MICP reaction process, bacterial urease hydrolysis provided a large amount of CO_3^{2-} and NH^{4+}, which rapidly increased the conductivity of the solution. In addition, a large amount of CO_3^{2-} and Ca^{2+} in the solution rapidly combined to form $CaCO_3$, resulting in a milky suspended substance in the solution. The suspended material gradually precipitated under the action of mineral nucleation. According to the zeta potential analysis shown in Figure 10, the addition of BL and SSP BL resulted in the absorption of calcium ions in the SSP solution, causing negative charges on the cell surfaces. Carbonate ions formed after the hydrolysis of urea, and these calcium ions formed the calcium carbonate precipitate, which coated the bacteria. As the reaction progressed, crystals composed of bacteria and calcium carbonate were gradually deposited at the bottom of the solution due to gravity.

3.2.5. Influence of Bacteria on Urea Hydrolysis in Different Culture Environments. Additional tests were conducted to further analyze the influence of BL, SSP BL, and FA BL on the conductivities of the FA and SSP solutions and characterize the continuous decomposition of urea in the FA and SSP solutions. In the test, 1 mL of the corresponding bacterial solution and 0.9 g urea were added to 9 mL of the corresponding solution, and the conductivity of the solution was tested for 72 h according to the conductivity method.

Figure 11 shows the test results that indicated that the conductivities of all solutions showed a gradual increase and essentially reached their maximum value at 50 h, after which

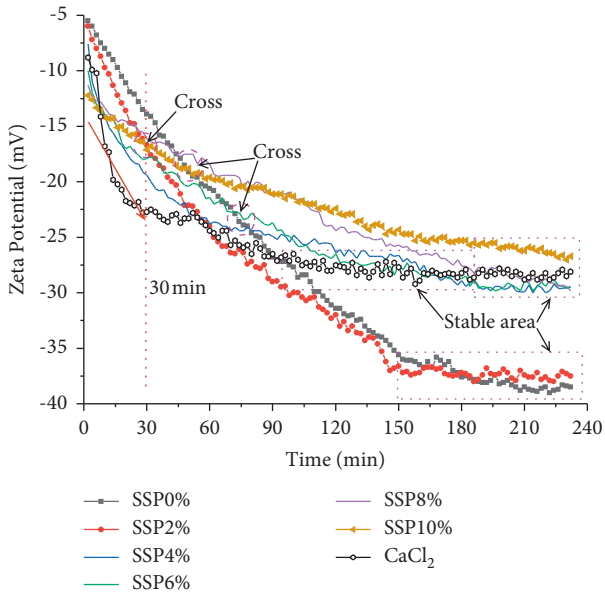

Figure 10: Zeta potential change graph.

they became mostly flat. The conductivities of BL and FA BL in the FA solution changed rapidly within 5 h, and overall conductivity was greater than in the SSP solution. The conductivity of BL and SSP BL in the SSP solution slowly changed in the first 5 h and then rapidly increased. The final conductivity difference between the FA and SSP solutions was 10 ms. The electrical conductivity of the bacteria in SSP was lower than FA, and the electrical conductivity of SSP increased slowly within the first 5 h, and it showed a significant increase after 5 h. However, it was always lower than in FA.

According to Figures 4 and 6, the initial pH value of the SSP solution was about 12.6, and after adding the bacterial solution, the pH value gradually decreased to between 10.3 and 10.5. When the pH value of the bacterial living environment was around 9, bacterial activity was higher. The higher the pH value of SSP solution reduced the urease activity of bacteria; thus, its conductivity slowly changed during the early stage. In addition, as shown in Figure 4, the concentration of Ca^{2+} in the SSP solution was high, and the bacteria chelated with Ca^{2+} to generate $CaCO_3$. This process reduced the concentration of conductive ions in the solution; therefore, the conductivity of the solution decreased within 5 min, as shown in Figure 5. During the continuous decomposition of urea by the bacteria, Ca^{2+} in the solution was gradually consumed, and the concentration of conductive ions in the solution gradually increased. After 5 h, the conductivity of the solution increased rapidly, indicating that Ca^{2+} was exhausted at this point.

3.2.6. Influence of Bacteria on the Calcium Carbonate Production and Yield in Different Culture Environments. To characterize the effects of bacteria in the different culture conditions on calcium carbonate production and yield, MICP aqueous solution curing efficiency tests were carried out with SSP BL, FA BL, and BL. The tests measured the curing effects of different bacteria in the aqueous solutions

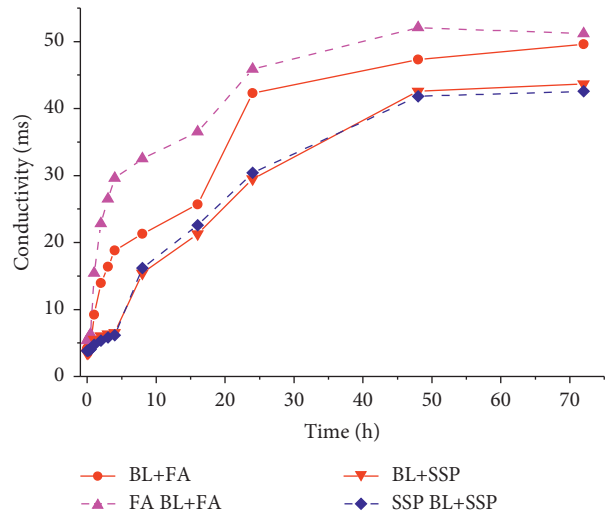

Figure 11: Long-term conductivity changes.

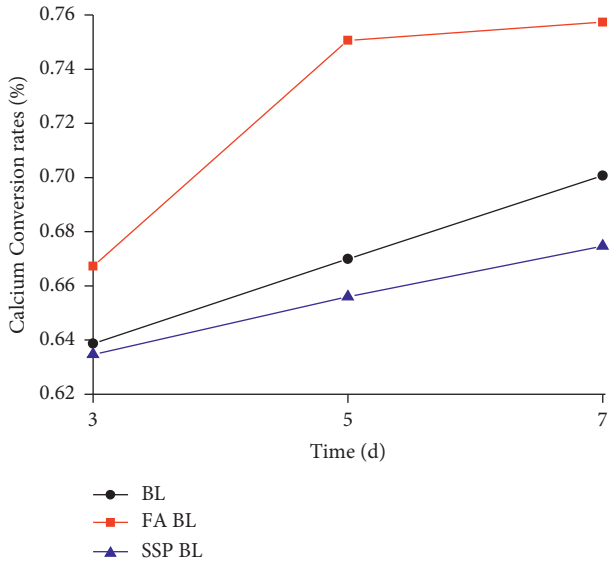

Figure 12: Efficiency of Ca^{2+} curing by different *Sporosarcina pasteurii*.

by calculating the calcium carbonate yield, and the tests were carried out using the acid wash method to calculate the amount of calcium carbonate produced [34]. Three milliliter of 3 bacterial solutions with an OD_{600} value of 2.0 were dropped into 30 mL of 0.5 M curing solution and tested for calcium carbonate production after 3, 5, and 7 d. The test results are shown in Figure 12.

As shown in Figure 12, the solution calcium carbonate yield of the bacteria under the three culture conditions increased with prolonged reaction time. The yield of $CaCO_3$ in the FA BL solution was the highest, while the yield of $CaCO_3$ reached 75% after 5 d. The yield of BL and SSP BL calcium carbonate also increased steadily with prolonged reaction time; however, the yield of $CaCO_3$ was lower than FA BL, reaching 70% and 67% after 7 d, respectively. The above test results showed that the efficiency of Ca^{2+} transformation of bacteria under different culture conditions was different and that FA BL had the highest yield.

S. pasteurii could grow at a pH of 7.0–9.0 and even as high as 12.0 in the FA and SSP solutions. Thus, it was necessary to carry out adaptive domestication of *S. pasteurii* in a high alkaline environment. In this work, BL was cultured in the FA and SSP solutions, and the urease activity and calcium carbonate yield of the domesticated bacteria in the FA and SSP solutions were analyzed by experimentation.

Figure 8 shows that the growth characteristics of *S. pasteurii* under different culture conditions were similar, and the OD_{600} value of FA BL cultured in the FA solution was higher. This indicated that the FA BL bacteria proliferated more under the same conditions. According to the comprehensive analysis shown in Figures 9, 11, and 9, the FA BL urease activity, long-term conductivity, and calcium carbonate yield were significantly higher than the other bacteria. The results showed that FA BL exhibited obvious adaptability after one acclimation, with a 55% increase in urease activity, 27% increase in long-term conductivity, and 7% increase in calcium carbonate yield. Thus, the SSP BL obtained after one acclimation was close to BL.

3.3. Nucleation of Ca^{2+} in Steel Slag Solutions on Bacterial Surfaces. Zeta potential measures the strength of mutual repulsion or attraction between particles, where the smaller the molecule or dispersed particle, the higher the absolute value of the potential (positive or negative). Thus, the more stable the system, the less likely it is to agglomerate [35]. Conversely, a lower zeta potential (positive or negative) would increase the likelihood that the solution would condense or coalesce, and the attractive force would exceed the repulsive forces; thus, dispersion would be hindered, and condensation or coalescence would occur. The relationship between the zeta potential and the stability of the system can be defined as follows [36]. Rapid condensation or coalescence will occur at a zeta potential of 0 to ±5 mV, and the solution will start to become unstable at ±10 to ±30 mV. At ±30 to ±40 mV, the solution will exhibit average stability, at ±40 to ±60 mV the solution will exhibit good stability, and above +61 mV, the solution will have excellent stability.

The charged nature of the colloid caused a two-electron layer structure to form on the surface of the colloid, and this structure affected the stability of the particles and their ability to aggregate and sink. The electrically charged nature of *S. pasteurii* also caused the surface to exhibit the same two-electron layer structure (money), due to the binding of *S. pasteurii* to Ca^{2+} by adsorption, which gradually formed an immobilized layer at the *S. pasteurii*-Ca^{2+} interface. These adsorbed ions formed the outer surface of the immobilized layer at the periphery of the bacteria, corresponding to a potential that could react with the zeta potential [37].

In this experiment, the zeta potential of bacteria was tested using the DT310 potentiometric analyzer, which utilized electroacoustics to characterize the adsorption of Ca^{2+} by *S. pasteurii* in the SSP solution by analyzing the changes in potential. This experiment was carried out at a temperature of 25°C. The SSP BL bacterial solution with an OD_{600} value of 2.0 was mixed with the SSP0–10% solutions and $CaCl_2$ (solution concentration was the same Ca^{2+} concentration of 30.5 mmol/L as SSP10% solution) solution at a ratio of 1:4. Then, the solution was placed into the potential analyzer, and the zeta potentials of each mixed solution were recorded at 2 min intervals. The concentration of Ca^{2+} in the FA solution was low, and the data measured by the zeta potential was more stable; thus, it was not very meaningful for comparison.

Figure 10 shows that after the bacterial solution was added to the SSP solution containing urea, the absolute value of the zeta potential of each concentration of SSP solution increased, indicating that the stability of the solution gradually increased. The absolute zeta potential values of SSP0% and SSP2% also increased with time over 150 min, and the rate of increase was significantly higher than the other solutions. After 150 min, the potential value gradually stabilized, with a stable value in the range of 35–40 mv, indicating the general stability of the solutions. After 190 min, the potential value gradually stabilized, and the stable values were in the range of 25–30 mv, while the stability of the solution was relatively low. When the bacterium solution was added to the SSP0–10% solution during the test, flocculation of the solution showed different phenomena. The larger the content of steel slag, the faster and more flocculation that appeared in the solution. Thus, the zeta potential of the $CaCl_2$ solution increased the fastest; the absolute value of the potential occurred within 30 min; and it gradually stabilized after 90 min. Thus, the potential value was in the range of ±10 to ±30 mV after stabilization. This indicated that the $CaCl_2$ solution required the least amount of time for the potential value to stabilize, and the complex composition of the SSP solution affected the stability of the solution's potential value.

A cell membrane is a selective barrier to some chemicals and ions depending on its desired or undesired components [38]. In addition, the specific surface area of this structure can decrease with the accumulation of crystals around the cell [39]. The accumulation of specific substrates, ions, or crystals may affect a reduction in cell membrane permeability, resulting in partial or total disruption of extracellular carbonate ion production [22].

According to experiments showing a maximum negative value of −38.5 for the zeta potential of Ca^{2+} free bacterial solutions SSP0%. This is related to the fact that bacterial cells maintain a negative electrostatic surface charge when incubated at physiological pH [40]. Due to the electronegativity of the cells, the bacterial cells can provide a complement to the electronegativity of the cell surface, facilitating the accumulation and complexation of positive metal ions. In this way, one of the requirements for starting MICP is achieved while supporting the stoichiometric interaction of calcium ions with extracellularly produced carbonate ions [39].

The SSP solution contained metal cations such as Ca^{2+}, with greater Ca^{2+} content of the steel slag dose (as shown in Figure 13). The metal cations in the SSP solution gradually migrated to the negatively charged bacterial surface under the action of the bacteria, forming a double electron layer. The higher the concentration of cations such as Ca^{2+}, the more cations that were adsorbed by the bacteria; thus, the thickness of the two-electron layer increased [41], and the rate of adsorption precipitation in the solution increased. As shown in

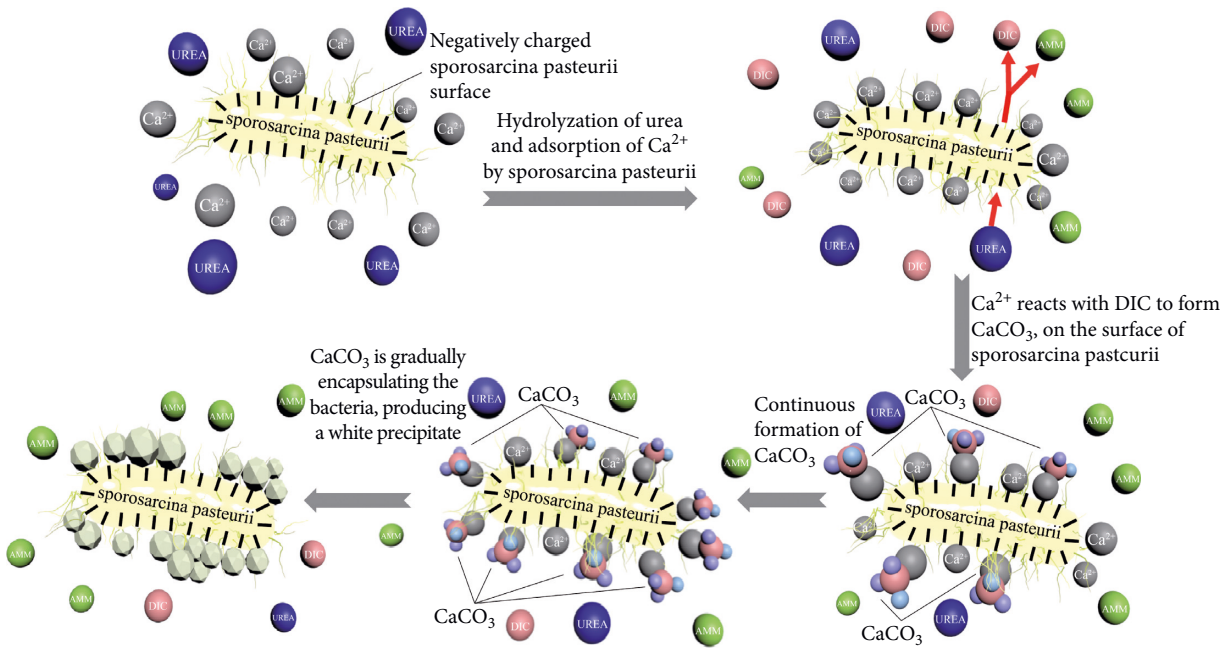

Figure 13: Nucleation process.

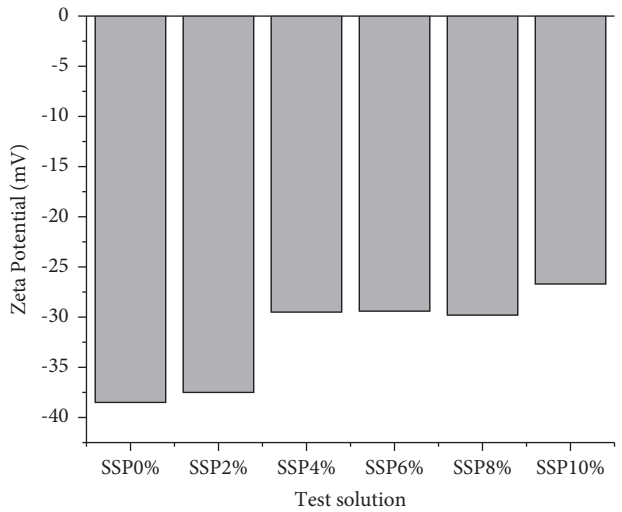

Figure 14: Solution potential graphs.

Figure 10, the change in potential from SSP4–10% indicated that the higher the Ca^{2+} content in the solution, the slower the change in potential, indicating that more cations were adsorbed by the bacteria. Therefore, a slower decrease in zeta potential in the solution indicated higher Ca^{2+} content and a thicker double electron layer of the bacteria, in addition to a longer stabilization duration. The zeta potential gradually stabilized after 190 min, indicating that Ca^{2+} in the solution was gradually depleted and the nucleation of minerals was stalled.

The initial adhesion of bacteria to the substrate is achieved through general physicochemical interactions such as van der Waals forces and electrostatic forces, through specific structures on the cell surface such as bacterial hairs and hyphae [39], and the electronegativity of the cell surface comes from reactive groups (e.g., carboxyl, phosphate, amino) [42]. Based on the zeta potential changes shown in Figure 10, it is clear that the rate of change is faster in the SSP0–2% solution, which has a very low Ca^{2+} content and less adsorption in the SSP2% solution. As shown in Figure 14, in the SSP4–10% solution, Ca^{2+} nucleated and aggregated at the cell surface, forming calcite crystals and reducing the permeability of the cell membrane. Compared to the Ca^{2+}-free bacterial solution, the total electronegativity of the SSP solution zeta potential all decreased to varying degrees, with the SSP10% solution showing the greatest decrease with a rate of 30.65%. The role of *Bacillus* sp. in providing nucleation sites for Ca^{2+} in mineral admixture solutions was further established based on the potential changes in the experimental results, thus providing some theoretical basis for the synergistic curing of mineral admixtures with microbially induced calcium carbonate precipitation.

4. Summary and Conclusions

In this study, a series of laboratory experiments were carried out on bacteria using pH tests, conductivity measurements, OD600 recordings, and zeta potential measurements to investigate the activity of bacteria in different mineral admixtures and the nucleation of minerals on the microbial surface to determine whether mineral admixtures and microorganisms can act synergistically to cure desert wind-deposited sands and to provide some theoretical support for later studies of the two working together to cure wind-deposited sands. The main findings are presented below:

(1) The activity of *S. pasteurii* differed in different mineral environments; the higher the mineral content, the higher the conductivity and pH values. Conductivity decreased during the initial stage when Ca^{2+} content was high. Bacteria had little effect on the pH value of the SSP solution but had a significant effect on the pH value of the FA solution. The results

showed that a higher pH value (>12) inhibited the urease activity of the bacteria.

(2) *S. pasteurii* showed good growth characteristics in the different mineral environments. Specifically, the bacteria in the FA environment showed a higher growth rate, hydrolysis efficiency, urease activity, and calcium carbonate yield, while the bacteria in the SSP environment performed normally.

(3) In the mineral admixture environment, Ca^{2+} nucleates and aggregates at the cell surface, forming calcite crystals that reduce the permeability of the cell membrane and the intercellular forces, reducing the overall electronegativity of the cells. Ca^{2+} concentration played an important role in the nucleation of mineral admixtures, where the higher the concentration of Ca^{2+}, the more noticeable the nucleation. In addition, when the Ca^{2+} concentration was below 15 mmol/L, nucleation was not apparent, defining the lower limit of nucleation of mineral admixtures.

(4) *S. pasteurii* showed high adaptability in the environment of steel slag and fly ash. When steel slag and fly ash were used as modified reinforcement materials, they played a synergistic role in curing the aeolian sand with microorganisms, providing a theoretical and experimental basis for the research and development of new sand-fixing materials and technologies.

Data Availability

The data used to support the findings of this study are available from the corresponding author upon request.

Conflicts of Interest

The authors declare that there are no conflicts of interest regarding the publication of this paper.

Acknowledgments

This research was supported by Xinjiang Regional Cooperative Innovation in Autonomous Region (2019E0241) and Hydraulic Engineering Key Discipline of Xinjiang Agricultural University (no. SLXK2019-05). Additional support was provided by the Postgraduate Research Innovation of Xinjiang Agricultural University, under project no. XJAUGRI2021013.

References

[1] A. Rao and H. Cölfen, "Mineralization and non-ideality: on nature's foundry," *Biophysical reviews*, vol. 8, no. 4, pp. 309–329, 2016.

[2] X. Y. Yang, B. Y. Wang, D. Cui, and L. Jia, "Physical and mechanical characters of sands in gurbantonggut desert," *Journal of Desert Research*, vol. 25, no. 4, pp. 563–569, 2005.

[3] B. Y. Ning, J. X. Ma, and Z. D. Jiang, "Influencing factors and conceptual model for suitability evaluation of ecological control technologies: an example in desertification control," *Journal of Desert Research*, vol. 40, no. 2, pp. 9–16, 2020.

[4] C. Li, S. H. Liu, T. J. Zhou, Y. Gao, and D. Yao, "The strength and porosity properties of micp-treated aeolian sandy soil," *Mechanics in Engineering*, vol. 39, no. 2, pp. 165–171, 2017.

[5] C. Qian, X. Yu, and X. Wang, "A study on the cementation interface of bio-cement," *Materials Characterization*, vol. 136, pp. 122–127, 2018.

[6] J. K. Mitchell and J. C. Santamarina, "Biological considerations in geotechnical engineering," *Journal of Geotechnical and Geoenvironmental Engineering*, vol. 131, no. 10, pp. 1222–1233, 2005.

[7] V. S. Whiffin, L. A. Van Paassen, and M. P. Harkes, "Microbial carbonate precipitation as a soil improvement technique," *Geomicrobiology Journal*, vol. 24, no. 5, pp. 417–423, 2007.

[8] M. G. Gomez, B. C. Martinez, J. T. DeJong, and C. E. Hunt, "Field-scale bio-cementation tests to improve sands," *Proceedings of the Institution of Civil Engineers - Ground Improvement*, vol. 168, no. 3, pp. 206–216, 2015.

[9] C. Li, D. Yao, S. Liu, and T. S. Y. L. Zhou, "Improvement of geomechanical properties of bio-remediated aeolian sand," *Geomicrobiology Journal*, vol. 35, no. 2, pp. 132–140, 2018.

[10] L. Cheng and R. Cord-Ruwisch, "Upscaling effects of soil improvement by microbially induced calcite precipitation by surface percolation," *Geomicrobiology Journal*, vol. 31, no. 5, pp. 396–406, 2014.

[11] M. J. Cui, J. J. Zheng, and H. J. Lai, "Experimental study of effect of particle size on strength of bio-cemented sand," *Rock and Soil Mechanics*, vol. 37, no. s2, pp. 397–402, 2016.

[12] L. Cheng, R. Cord-Ruwisch, and M. A. Shahin, "Cementation of sand soil by microbially induced calcite precipitation at various degrees of saturation," *Canadian Geotechnical Journal*, vol. 50, no. 1, pp. 81–90, 2013.

[13] J. T. DeJong, B. M. Mortensen, B. C. Martinez, and D. C. Nelson, "Bio-mediated soil improvement," *Ecological Engineering*, vol. 36, no. 2, pp. 197–210, 2010.

[14] F. G. Ferris, V. Phoenix, Y. Fujita, and R. W. Smith, "Kinetics of calcite precipitation induced by ureolytic bacteria at 10 to 20°C in artificial groundwater," *Geochimica et Cosmochimica Acta*, vol. 68, no. 8, pp. 1701–1710, 2004.

[15] Y. Zhou, H. J. Zhou, and C. M. Zhou, "Exploration of hydrogen sources for the low-carbon and green production in the steel industry in China," *Chemical Industry and Engineering Progress*, vol. 41, no. 2, pp. 1073–1077, 2022.

[16] Q. Jin, L. Zhu, J. Madiniyeti, C. He, and L. Li, "Influence of active inorganic fillers on the physical and mechanical properties of polyvinyl chloride wood-plastic composites when immersed," *Bioresources*, vol. 16, no. 1, pp. 789–804, 2020.

[17] X. Y. He, K. F Zhang, W. Yang, X. Wu, and Y. Ming, "Development on applications of silicate solid wastes as concrete admixture," *Materials Review*, vol. 27, no. S1, pp. 281–284, 2013.

[18] L. Zhao, Z. J. Tang, and F. Liu, "Laboratory tests of fly ash as a sandy soil amendment and its effects on soil water," *Acta Scientiae Circumstantiae*, vol. 29, no. 9, pp. 1951–1957, 2009.

[19] V. C. Pandey and N. Singh, "Impact of fly ash incorporation in soil systems," *Agriculture, Ecosystems & Environment*, vol. 136, no. 1-2, pp. 16–27, 2010.

[20] I. Akinwumi, "Soil modification by the application of steel slag," *Periodica Polytechnica: Civil Engineering*, vol. 58, no. 4, pp. 371–377, 2014.

[21] L. Huang, Z. Peng, C. Lu, Y. Chen, J. W. Lv, and M. D. Qin, "Ginsenoside Rg1 alleviates repeated alcohol exposure-induced psychomotor and cognitive deficits," *Chinese Medicine*, vol. 15, no. 1, pp. 44–52, 2020.

[22] O. Šovljanski, L. Pezo, A. Tomić, A. Ranitović, and D. S. Cvetković, "Contribution of bacterial cells as nucleation centers in microbiologically induced CaCO 3 precipitation-A mathematical modeling approach," *Journal of Basic Microbiology*, vol. 61, no. 9, pp. 835–848, 2021.

[23] N. W. Soon, L. M. Lee, T. C. Khun, and H. S. Ling, "Factors affecting improvement in engineering properties of residual soil through microbial-induced calcite precipitation," *Journal of Geotechnical and Geoenvironmental Engineering*, vol. 140, no. 5, Article ID 04014006, 2014.

[24] A. C. Mitchell and F. G. Ferris, "The influence ofBacillus pasteuriion the nucleation and growth of calcium carbonate," *Geomicrobiology Journal*, vol. 23, no. 3-4, pp. 213–226, 2006.

[25] K. Tian, Y. Wu, H. Zhang, and D. K. S. Li, "Increasing wind erosion resistance of aeolian sandy soil by microbially induced calcium carbonate precipitation," *Land Degradation & Development*, vol. 29, no. 12, pp. 4271–4281, 2018.

[26] V. S. Whiffin, *Microbial CaCO3 Precipitation for the Production of Biocement*, Murdoch University, Western Australia, 2004.

[27] S. Zhou, *Modern Microbial Biotechnology"*, Higher Education Press, China, 2007.

[28] M. Pansu and J. Gautheyrou, *pH Measurement"*, Springer Berlin Heidelberg, Berlin/Heidelberg, Germany, 2006.

[29] A. A. Elseewi, A. L. Page, and S. R. Grimm, "Chemical characterization of fly ash aqueous systems," *Journal of Environmental Quality*, vol. 9, no. 3, pp. 424–428, 1980.

[30] W. M. Mayes, P. L. Younger, and J. Aumônier, "Hydrogeochemistry of alkaline steel slag leachates in the UK," *Water, Air, and Soil Pollution*, vol. 195, no. 1-4, pp. 35–50, 2008.

[31] C. X. Qian and X. Zhang, *New Biocement"*, Science Press, China, 2019.

[32] D. Gat, M. Tsesarsky, and D. Shamir, "Ureolytic calcium carbonate precipitation in the presence of non-ureolytic competing bacteria," *Geo-Frontiers*, vol. 5, pp. 3966–3974, 2011.

[33] D. Gat, M. Tsesarsky, D. Shamir, and Z. Ronen, "Accelerated microbial-induced $CaCO_3$ precipitation in a defined coculture of ureolytic and non-ureolytic bacteria," *Biogeosciences*, vol. 11, no. 10, pp. 2561–2569, 2014.

[34] Q. Zhao, *Experimental Study of Microbially Induced Calcium Carbonate Precipitation (MICP) for Soil Consolidation*, China University of Geosciences (Bei Jing), China, 2014.

[35] C. X. Qian, X. Zhang, and H. H. Yi, "Effect and mechanism of microorganism to improve the stability and strength of steel slag cementitious material," *Bulletin of The Chinese Ceramic Society*, vol. 39, no. 8, pp. 2363–2371, 2020.

[36] L. W. Mo, F. Zhang, M. Deng, F. Jin, A. Al-Tabbaa, and A. Wang, "Accelerated carbonation and performance of concrete made with steel slag as binding materials and aggregates," *Cement and Concrete Composites*, vol. 83, pp. 138–145, 2017.

[37] Z. Zheng and L. Ning, *Molecular Forces and Colloidal Stabilisation and Agglomeration"*, Higher Education Press, China, 1995.

[38] R. Fettiplace and D. A. Haydon, "Water permeability of lipid membranes," *Physiological Reviews*, vol. 60, no. 2, pp. 510–550, 1980.

[39] T. Zhu and M. Dittrich, "Carbonate precipitation through microbial activities in natural environment, and their potential in biotechnology: a review," *Frontiers in Bioengineering and Biotechnology*, vol. 4, no. 4, 2016.

[40] W. E. Krumbein, "Bacterial calcification," *Microbial Sediments*, Springer, Berlin, Heidelberg, pp. 25–31, 2000.

[41] F. F. Min, Q. Zhao, H. L. Li, and C. L. Peng, "Study of electrokinetic properties of kaolinite in coal slime," *Journal of China University of Mining & Technology*, vol. 42, no. 2, pp. 284–290, 2013.

[42] E. Kłodzińska, M. Szumski, E. Dziubakiewicz, and K. E. W. B. Hrynkiewicz, "Effect of zeta potential value on bacterial behavior during electrophoretic separation," *Electrophoresis*, vol. 31, no. 9, pp. 1590–1596, 2010.